New results for delayed neural field equations

Grégory Faye, Olivier Faugeras

New results for delayed neural field equations

Grégory Faye[1] and Olivier Faugeras[1]

[1] NeuroMathComp Laboratory, INRIA Sophia Antipolis, CNRS, ENS Paris,
2004 Route des Lucioles-BP 93 FR-06902 Sophia Antipolis,
France,
gregory.faye@sophia.inria.fr olivier.faugeras@sophia.inria.fr

May 6, 2010

Abstract

Neural field models with delays define a useful framework for modeling macroscopic parts of the cortex involving several populations of neurons. Nonlinear delayed integro-differential equations describe the spatio-temporal behavior of these fields. Using methods from the theory of delay differential equations, we show the existence and uniqueness of a solution of these equations. A Lyapunov analysis gives us sufficient conditions for the solutions to be asymptotically stable. We also present a study of the numerical computation of these solutions in a special case. This is, to our knowledge, the first time that a serious analysis of the problem of the existence and uniqueness of a solution of these equations has been performed. Another original contribution of ours is the definition of a Lyapunov functional and the result of stability it implies. We illustrate our work on a variety of examples that are relevant to modeling in neuroscience.

Keywords: Neural fields; nonlinear integro-differential equations; delays; Lyapunov functional; pattern formation; numerical schemes.

1 Introduction

Delays arise naturally when we model neurobiological systems. For example, the finite-velocity propagation of action potentials, or the dendritic and synaptic processing can generate delays on the order of milliseconds. Effective delays can also be induced by the spike-generation dynamics. First, the delay due to propagation of action potentials along the axon depends on the travelled distance as well as on the type of neurons. Indeed, conduction velocities in the axon can range from about $1m.s^{-1}$ along unmyelinated axons to more than $100m.s^{-1}$ along myelinated ones. This is one of the reasons why significant time delays can emerge in certain brain structures. Second, some cells may have synapses or gap junctions on dendrites far from the cell body. In this case, there can also be a delay associated with the propagation of the action potential along the dendrite. Another delay can occur at a synaptic contact point in the transduction of an electrical signal into a biochemical signal and back again to a post-synaptic potential. Hence, the growing interest in understanding network models with space-dependent delays [2, 3, 4, 7, 8, 9].

In this work, we focus on space-dependent delays. In particular we incorporate delays in the well-known Wilson and Cowan [10, 11] and Amari [1] models for neural fields. In order to cover both axonal and dendritic delays and contrary to most of the papers on the subject, we deal with very general delay integro-differential equations without specifying the form of the delays.

We present a general mathematical framework for the modeling of neural fields which is based on tools of delay-differential equation analysis and an original presentation and analysis of numerical schemes. We illustrate our results with numerical experiments.

2 The models

Neural fields are continuous networks of interacting neural masses, describing the dynamics of the cortical tissue at the population level. These neural field models of population firing rate activity can be described, when delays are not taken into account by the following integro-differential equations:

$$\partial_t \mathbf{V}(r,t) = -L\mathbf{V}(r,t) + \int_\Omega \mathbf{W}(r,r',t)\mathbf{S}(\mathbf{V}(r',t))dr' + I_{\text{ext}}(r,t) \tag{1}$$

Let us briefly describe the various elements that appear in this equation before extending it to the case of delays.

We consider n interacting populations of neurons whose state is described by their membrane potential $\mathbf{V}$, a vector of dimension n. The function $\mathbf{S} : \mathbb{R}^n \to \mathbb{R}^n$ is defined by $\mathbf{S}(x) = [S_1(x_1), \dots, S_n(x_n)]^T$ where S_i is sigmoidal. The functions S_i satisfy the properties introduced in the following definition:

Definition 2.1. *For all $i = 1, \dots, n$ S_i and S_i' are positive and bounded (S_i' is the derivative of the function S_i). We note $S_{im}' = \sup_x S_i'(x)$, $S_m = \max_i \sup_x S_i(x)$ and $DS_m = \max_i S_{im}'$. Finally we define $D\mathbf{S}$ as the diagonal matrix* $\text{diag}(S_i')$.

The relation between the firing rate ν_i of population i and its membrane potential V_i is given by the relation $\nu_i = S_i(V_i)$.

The neuronal populations are distributed over some continuum, a bounded open subset Ω of $\mathbb{R}^q$, $q = 1, 2, 3$. The variables r and r' in (1) belong to Ω. The $n \times n$ matrix L is assumed to be diagonal, $L = \text{diag}(l_1, \cdots, l_n)$, where the positive number l_i characterize the dynamics of the ith population, $i = 1, \cdots, n$. The $n \times n$ matrix function $\mathbf{W}(r, r', t)$ describes how the populations at point r' influence those at point r at time t. More precisely, $W_{i,j}(r, r', t)$ describes how population j at point r' influences population i at point r at time t. Finally $I_{\text{ext}}(r, t)$ is an external current that models external sources of excitation.

It is now straightforward to extend (1) to take into account space dependent delays. We introduce the n-dimensional vector function $\mathbf{d}(r, r')$ and assume its components to be non negative. $d_i(r, r')$ is the time it takes for the information about the ith population at location r' to reach the populations at location r. Having said this we rewrite (1) as follows

$$\partial_t \mathbf{V}(r,t) = -L\mathbf{V}(r,t) + \int_\Omega \mathbf{W}(r,r',t) \times \mathbf{S}(\mathbf{V}(r', t - \mathbf{d}(r,r')))dr' + I_{\text{ext}}(r,t) \quad (2)$$

3 Existence and uniqueness of a solution

In this section we deal with the problem of the existence and uniqueness of a solution to (2) for a given initial condition. We first introduce the framework in which this equation makes sense.

We start with the assumption that the state vector $\mathbf{V}$ is a differentiable (resp., square integrable) function of the time (resp. the space) variable. Let Ω be an open subset of $\mathbb{R}^q$ where $q = 1, 2, 3$ and $\mathcal{F}$ be the set $L^2(\Omega, \mathbb{R}^n)$ of the square integrable functions from Ω to $\mathbb{R}^n$. The Fischer-Riesz's theorem ensures that $\mathcal{F}$ is a Banach space. We denote by $\mathcal{I}$ an interval of $\mathbb{R}$ containing 0.

3.1 The well-posedness of (2)

We define the Banach space $\mathcal{C} = \mathcal{C}([-d, 0], \mathcal{F})$ of the continuous functions from $[-d, 0]$ to $\mathcal{F}$ where $d = \sup_{\overline{\Omega}\times\overline{\Omega}} \mathbf{d}$. We use the traditional notation introduced by Hale in [6]:

$$\mathbf{X}_t(\theta) = \mathbf{X}(t + \theta) \quad \theta \in [-d, 0]$$

when $\mathbf{X}_t \in \mathcal{C}$ for all $t \geq 0$. Equation (2) is formally recast as a retarded functional differential equation on the Banach space $\mathcal{F}$ with initial value $\phi \in \mathcal{C}$:

$$\begin{cases} \dot{\mathbf{V}}(t) = f(t, \mathbf{V}_t) \\ \mathbf{V}_0 = \phi \end{cases} \quad (3)$$

where $\mathbf{V}(t)$ is thought of as a mapping $\mathbf{V} : \mathcal{I} \to \mathcal{F}$. This means that $\mathbf{V}(t)$ is a function defined in Ω by $\mathbf{V}(t)(r) = \mathbf{V}(r, t)$, similarly we have $\mathbf{V}_t(\theta)(r) = \mathbf{V}(r, t + \theta)$. The function f from $\mathcal{I} \times \mathcal{C}$ is equal to the righthand side of (2):

$$f(t, \mathbf{V}_t)(r) = -L\mathbf{V}_t(r, 0) + \int_\Omega \mathbf{W}(r, r', t)\mathbf{S}(\mathbf{V}_t(r', -\mathbf{d}(r, r')))dr' + I_{\text{ext}}(r, t) \quad \forall t \geq 0 \quad \forall r \in \Omega$$

We define by $\bar{\Omega}$ the closure of Ω.

Lemma 3.1. *If the following assumptions are satisfied:*

- $W \in \mathcal{C}(\mathbb{R}, L^2(\Omega^2, \mathcal{M}_n(\mathbb{R})))$,
- $\mathbf{d} \in \mathcal{C}(\bar{\Omega}^2, \mathbb{R}^n_+)$,
- *the external current* $I_{ext} \in \mathcal{C}(\mathcal{I}, \mathcal{F})$,

then f is well defined and is from $\mathcal{I} \times \mathcal{C}$ to $\mathcal{F}$.

Proof. See [5]. □

3.2 Existence and uniqueness of a solution

Let $\mathcal{I} = [0, +\infty[$. The following theorem ensures existence and uniqueness of a solution of (2) on $[-d, +\infty[$.

Theorem 3.1. *If the following hypotheses are satisfied:*
- $W \in \mathcal{C}(\mathcal{I}, L^2(\Omega^2, \mathcal{M}_n(\mathbb{R})))$,
- the external current $I_{ext} \in \mathcal{C}(\mathcal{I}, \mathcal{F})$,
- $\mathbf{d} \in \mathcal{C}(\bar{\Omega}^2, \mathbb{R}^n_+)$,
Then for any $\phi \in \mathcal{C}$, there exists a unique solution $\mathbf{V} \in \mathcal{C}^1([0, +\infty[, \mathcal{F}) \cap \mathcal{C}([-d, +\infty[, \mathcal{F})$.

Proof. See [5]. □

4 Linear stability analysis in the autonomous case

The aim of this section is to work at a fixed point $\mathbf{V}^0$ of (2) and study a linear retarded functional differential equation. The theory introduced by Hale in [6] is based on autonomous systems, this is why we need to impose that the connectivity does not depend on the time t, we note $\mathbf{W}(r, r')$.

4.1 The linearization

Let $\mathbf{V}^0$ be a fixed point of (2), *i.e.* $\mathbf{V}^0$ satisfies:

$$0 = -L\mathbf{V}^0(r) + \int_\Omega \mathbf{W}(r, r')\mathbf{S}(\mathbf{V}^0(r'))dr' + I_{\text{ext}}(r) \quad \forall r \in \Omega$$

We define a new connectivity:

$$\forall (r, r') \in \Omega^2 \quad \widetilde{\mathbf{W}}(r, r') = \mathbf{W}(r, r') \cdot D\mathbf{S}(\mathbf{V}^0(r'))$$

Proposition 4.1. *Let Ω be an open set and $\boldsymbol{W} \in L^2(\Omega^2, \mathcal{M}_n(\mathbb{R}))$ then $\widetilde{\boldsymbol{W}} \in L^2(\Omega^2, \mathcal{M}_n(\mathbb{R}))$.*

We are now able to define on $\mathcal{F}$ the linearized equation around $\mathbf{V}^0$:

$$\partial_t \mathbf{U}(r,t) = -L\mathbf{U}(r,t) + \int_\Omega \widetilde{\mathbf{W}}(r,r')\mathbf{U}(r',t-\mathbf{d}(r,r'))dr' \quad \forall t \geq 0 \quad \forall r \in \Omega \quad (4)$$

If 0 is asymptotically stable for (4) then $\mathbf{V}^0$ is also asymptotically stable for (2). This result, already known in finite dimensions, is non trivial to establish in infinite dimensions because it requires the study of the characteristic values of the infinitesimal generator associated to (4).

4.2 Stability by the method of Lyapunov functionals

We now introduce a Lyapunov function for equation (4) in order to study the stability of the 0 solution.

Rescaling the equation In order to establish a stability bound, we rescale equation (4) by $\frac{t}{\lambda}$ where λ is a parameter which will be chosen later. Equation (4) becomes:

$$\partial_t \mathbf{U}(r,t) = -\lambda L\mathbf{U}(r,t) + \lambda \int_\Omega \widetilde{\mathbf{W}}(r,r') \times \mathbf{U}(r',t-\frac{\mathbf{d}(r,r')}{\lambda})dr' \quad \forall t \geq 0 \quad (5)$$

Definition of the Lyapunov functional We now introduce the Lyapunov functional that will allow us to conclude on the stability of (5). We use the notation introduced in the previous section, $\mathbf{U}_t$ means that, for all $t \geq 0$ we have $\mathbf{U}_t(\theta) = \mathbf{U}(t+\theta)$ for all $\theta \in [-d, 0]$.

$$\mathcal{V}(\mathbf{U}_t) = \frac{1}{2}\sum_{i=1}^n \int_\Omega l_i^{-1} U_i(r,t)^2 dr + \int_\Omega \beta(r) \sum_{i=1}^n \int_\Omega \int_{-\frac{d_i(r,r')}{\lambda}}^0 U_i(r',t+\theta)^2 d\theta dr' dr$$

where $\beta \in L^1(\Omega, \mathbb{R})$ is defined below in (6).

$$\beta(r) = \sum_{i,j=1}^n \int_\Omega l_i^{-2} \widetilde{W}_{i,j}(r,r')^2 dr' \quad (6)$$

This leads us to the following proposition.

Proposition 4.2. *If* $\int_\Omega \beta(r)dr < \lambda - \frac{\lambda^2}{4}$ *then* $\dot{\mathcal{V}}(\mathbf{U}_t) < -\epsilon \sum_{i=1}^n \int_\Omega U_i(r,t)^2 dr$,
where $\epsilon = \lambda - \frac{\lambda^2}{4} - \int_\Omega \beta(r)dr$.

The result If $\mathbf{W}$ belongs to $L^2(\Omega^2, \mathcal{M}_n(\mathbb{R}))$, we define its norm by:

$$\|\mathbf{W}\|_F = \sqrt{\sum_{i,j=1}^n \int_\Omega \int_\Omega W_{i,j}(r,r')^2 dr' dr}$$

Theorem 4.1. *If* $\|L^{-\frac{1}{2}} \widetilde{\boldsymbol{W}} L^{-\frac{1}{2}}\|_F < 1$ *then* $\boldsymbol{V}^0$ *is uniformly asymptotically stable.*

Proof. See [5]. □

4.3 Discussion of the bound

We have presented a method which gives a bound for the asymptotic stability. To our knowledge, Wu in [12] was the first to establish a bound of stability for general retarded functional differential equations. In our notations his bound can be written $\|\widetilde{\mathbf{W}}\|_F < \ell e^{-\ell d}$ which has the advantage to take into account the delays but has also the disadvantage to be very conservative (where $\ell \stackrel{def}{=} \min_i l_i$). Atay and Hutt in [2] find a bound in the case of a one population equation, with $\Omega = \mathbb{R}$. We can recover a similar bound in our framework by changing the form of β by choosing $\beta(r) = \sum_{i,j=1}^n \int_\Omega \ell^{-2} \widetilde{W}_{i,j}(r,r')^2 dr'$ and so if $\|\widetilde{\mathbf{W}}\|_F < \ell$ then $\mathbf{V}^0$ is asymptotically stable. This shows that this bound is better than the one obtained by Wu. Finally we see that our bound $\|L^{-\frac{1}{2}} \widetilde{\mathbf{W}} L^{-\frac{1}{2}}\|_F < 1$ obtained by the method of Lyapunov functional is the less conservative.

5 Numerical simulations

The aim of this section is to numerically solve equation (2) for different n and q. We remind the reader that n is the number of populations of neurons and q is the spatial dimension. This implies developing a numerical scheme that approaches the solution of our equation, and to prove that this scheme effectively converges to the solution. Several computer codes have been developed in the last decades for the numerical integration of functional differential equations. **dde23**, written in **Matlab**, can efficiently solve delay differential equations with constant delays. We decided to make it the center of our numerical investigation. The main motivation of this choice was that this solver can deal with delay equations with a large number of constant delays. This turns out to be a big advantage, as shown later.

5.1 Two populations of neurons in 1D

We consider two (n=2) one-dimensional (q=1) populations of neurons, population 1 being excitatory and population 2 being inhibitory. We have the following equations:

$$\begin{cases} \partial_t v_1(x,t) = -\alpha_1 v_1(x,t) \\ + \int_{-1}^1 \left[w_{1,1}(x-y) S_1\big(v_1(y, t-\frac{|x-y|}{c_1})\big) \right. \\ \left. + w_{1,2}(x-y) S_2\big(v_2(y, t-\frac{|x-y|}{c_2})\big)\right] dy \\ \partial_t v_2(x,t) = -\alpha_2 v_2(x,t) \\ + \int_{-1}^1 \left[w_{2,1}(x-y) S_1\big(v_1(y, t-\frac{|x-y|}{c_1})\big) \right. \\ \left. + w_{2,2}(x-y) S_2\big(v_2(y, t-\frac{|x-y|}{c_2})\big)\right] dy \end{cases} \quad (7)$$

We assume for simplicity that:

Hypothesis 5.1.

$$\alpha_1 = \alpha_2 = \alpha \quad c_1 = c_2 = c$$
$$S_1(x) = S_2(x) = S(x)$$
$$w_{i,j}(x) = \frac{a_{i,j}}{\sqrt{2\pi\sigma_{i,j}^2}} e^{-\frac{x^2}{2\sigma_{i,j}^2}} \quad a_{i,2} \leq 0,\ a_{i,1} \geq 0,\ i = 1,2 \quad (8)$$

Definition 5.1. *Let E_u and E_d be the following two matrices in $\mathcal{M}_{m+1}(\mathbb{R})$:*

$$E_u = \begin{pmatrix} 0 & 1 & 0 & \dots & 0 \\ \vdots & \ddots & \ddots & \ddots & \vdots \\ \vdots & (0) & \ddots & \ddots & 0 \\ \vdots & (0) & (0) & \ddots & 1 \\ 0 & \dots & \dots & \dots & 0 \end{pmatrix} \qquad E_d = E_u^T$$

We then define $\forall k = 1, \dots, m$

$$E_k = E_0(E_u^k + E_d^k),$$

$$\text{with } E_0 = \begin{pmatrix} \frac{1}{2} & 0 & \dots & \dots & 0 \\ 0 & 1 & \ddots & (0) & 0 \\ \vdots & \ddots & \ddots & \ddots & \vdots \\ \vdots & (0) & \ddots & 1 & 0 \\ 0 & \dots & \dots & 0 & \frac{1}{2} \end{pmatrix}.$$

We use the trapezoidal rule and denote by $v_1^i(t)$ (resp. $v_2^i(t)$) the approximation $v_1(x_i, t)$ (resp. $v_2(x_i, t)$). $V_1(t)$ (resp. $V_2(t)$) is the vector of length $m+1$ with components $v_1^i(t)$ (resp. $v_2^i(t)$).

We obtain the following numerical scheme:

$$\frac{dV_1}{dt}(t) = -\alpha V_1(t) + h\sum_{k=0}^{m}\big[w_{1,1}(kh)E_k\widetilde{\mathbf{S}}\big(V_1(t-\frac{kh}{c}) + w_{1,2}(kh)E_k\widetilde{\mathbf{S}}\big(V_2(t-\frac{kh}{c})\big]$$

$$\frac{dV_2}{dt}(t) = -\alpha V_2(t) + h\sum_{k=0}^{m}\big[w_{2,1}(kh)E_k\widetilde{\mathbf{S}}\big(V_1(t-\frac{kh}{c}) + w_{2,2}(kh)E_k\widetilde{\mathbf{S}}\big(V_2(t-\frac{kh}{c})\big],$$

where $\widetilde{\mathbf{S}} : \mathbb{R}^n \to \mathbb{R}^n$ is defined by $\widetilde{\mathbf{S}}(x) = [S(x_1), \dots, S(x_n)]^T$.

We now present different numerical examples. For each example we fix the nonlinearity S to be:

$$S(x) = \frac{1}{1+e^{-\mu x}} - \frac{1}{2} \tag{9}$$

5.1.1 Absolute stability

We begin our numerical experiments with an example of the stability result established by the method of Lyapunov functionals in section 4.2. The values of the parameters

$$\mathcal{A} = (a_{i,j}) = \begin{pmatrix} 2 & -\sqrt{2} \\ \sqrt{2} & -2 \end{pmatrix}, \quad \Sigma = (\sigma_{i,j}) = \begin{pmatrix} 1 & 0.1 \\ 0.1 & 1 \end{pmatrix} \tag{10}$$

yield $\|\tilde{W}\|_F = 0.757$. If we choose $\alpha = 1$ and $\mu = 1$ then the condition of theorem 4.1 is satisfied; hence the homogeneous solution $V = 0$ is uniformly asymptotically stable (absolutely stable) as we can see in figure (1) . The initial conditions are drawn randomly.

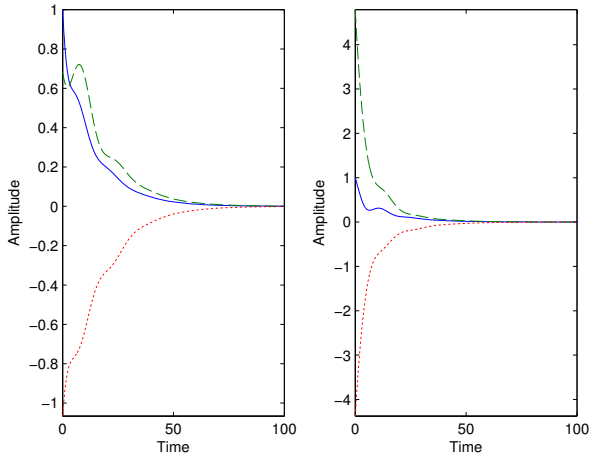

Figure 1: An illustration of the absolute stability of the fixed point at the origin: the trajectories of the state vector converge to a single trajectory, independently of the choice of the initial function. Results are shown for the neural mass of spatial coordinate: 0. Left: population 1. Right: population 2. The three curves correspond to three different initial conditions. The velocity is $c = 0.2$.

5.1.2 Effect of the slope μ on the solutions, loss of absolute stability

We next study the effect of increasing the slope of the sigmoid. In each experiment the initial conditions are the same. We present the case corresponding to the values of the parameters shown in (10). We observe that increasing the slope from $\mu = 1$ to $\mu = 3$ drastically changes the behavior of the solution. For $\mu = 1$ the system is absolutely stable and, unsurprisingly, the solution simply converges to its homogenuous state $V = 0$, as shown in figure 2. For $\mu = 3$ the solution oscillates in time, as shown in figure 3. This could be caused by a Hopf bifurcation. In order to prove this assertion we would have to perform the bifurcation analysis with respect to the parameter μ which is outside the scope of this paper. Moreover, the condition of theorem 4.1 is not satisfied, so we have lost the absolute stability. Indeed with $\mu = 3$, we have $\|\tilde{W}\|_F = 2.271 \geq \frac{1}{5} = \alpha$.

5.2 One population of neurons in 2D

This section is devoted to the case of $\Omega =]-l, l[\times]-l, l[$ with $l > 0$.

We suppose that the connectivity function W is isotropic in the following sense

$$\forall r, r' \in \mathbb{R}^2 \quad W(r, r') = w(\|r - r'\|) \text{ and } d(x, y) = \frac{\|x-y\|}{c},$$

where $w : \mathbb{R}^+ \to \mathbb{R}$. We choose a connectivity function suggested by Amari in [1], commonly referred to as the "Mexican hat" connectivity. It features center excitation and surround inhibition which is an effective model for a mixed population of interacting inhibitory and excitatory

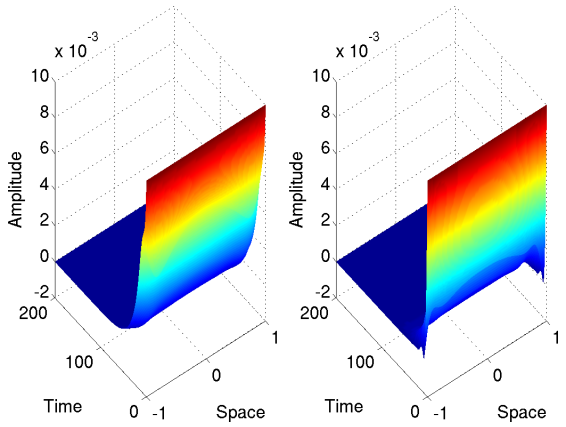

Figure 2: Effect of the slope on the solutions of equation (7) in the case of the parameters given by (10). Plots of population 1 (left) and population 2 (right). Parameters are: $\mu = 1$, $c = 0.2$, and $\alpha = \frac{1}{5}$.

neurons with typical cortical connections.

$$w(x) = \frac{1}{\sqrt{2\pi\xi_1^2}} e^{-\frac{\|x\|^2}{2\xi_1^2}} - \frac{A}{\sqrt{2\pi\xi_2^2}} e^{-\frac{\|x\|^2}{2\xi_2^2}}, \qquad (11)$$

with $0 < \xi_1 \leq \xi_2$ and $0 \leq A \leq 1$.
We choose for simplicity the following norm:

$$\forall r = (x, y) \in \mathbb{R}^2 \quad \|r\|_1 = \mid x \mid + \mid y \mid$$

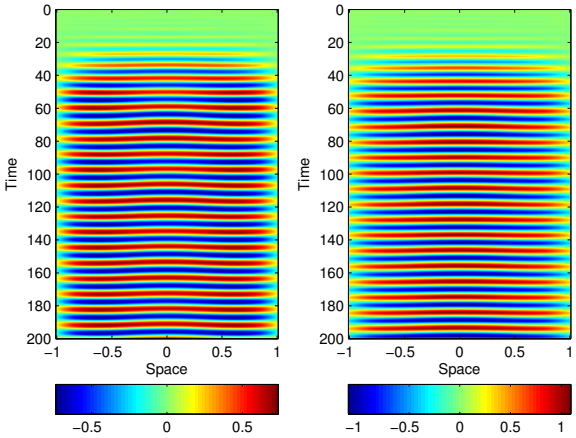

Figure 3: Effect of the slope on the solutions of equation (7) in the case of the parameters given by (10). Plots of population 1 (left) and population 2 (right). Parameters are: $\mu = 3$, $c = 0.2$, and $\alpha = \frac{1}{5}$.

The choice of this particular norm instead of the usual Euclidean norm is essentially guided by their relative computational requirements: it is easier to compute $\|\cdot\|_1$ than $\|\cdot\|_2$ on a square lattice, and the number of delays that appear in the discretization scheme is very sensitive to the choice of the norm since $d(x, y) = \frac{\|x-y\|}{c}$.

5.2.1 Purely excitatory connectivity

In these experiments we choose $\xi_1 = 0.3$ and $A = 0$ in (11). We fix $l = 1$ for Ω and use $m = 30$ for the discretization in space.

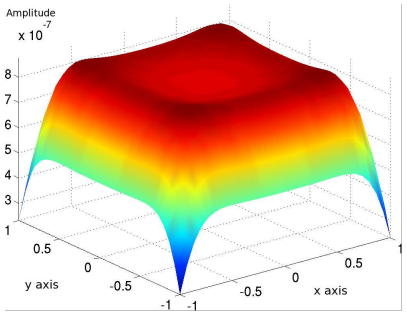

Figure 4: Plot of the solution of equation (2) at $T = 700$ for $n = 1$ and $q = 2$, for the values $\xi_1 = 0.3$ and $A = 0$ in (11) and for $\mu = 1$.

For $\mu = 1$ the system is absolutely stable and, unsurprisingly, the solution simply converges to its homogeneous state $V = 0$, as shown in figure 4. Increasing the slope from $\mu = 1$ to $\mu = 10$ changes the behavior of the solution. Indeed, in figure 5, almost all the network is excited, in agreement with the choice of a purely excitatory connectivity.

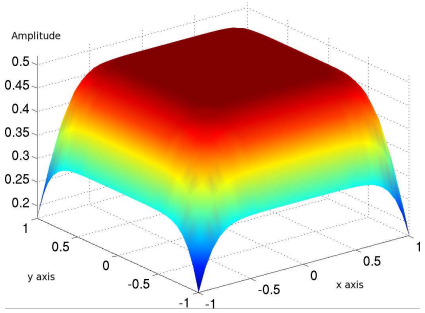

Figure 5: Plot of the solution of equation (2) at $T = 700$ for $n = 1$ and $q = 2$, for the values $\xi_1 = 0.3$ and $A = 0$ in (11) and for $\mu = 10$.

5.2.2 Mexican hat connectivity

We choose the connectivity $\xi_1 = 0.2$, $\xi_2 = 0.3$ and $A = 1$ in (11) in order to discover new patterns of activity. The corresponding solution at $T = 700$ is shown in figure 6 for the value 25 of the slope μ.

We observe the emergence of periodic square patterns that seem to indicate that the solution is converging toward a simple biperiodic pattern. This impression is confirmed by figure 7 where we plot the guessed function $(x, y) \mapsto \cos(7x)\cos(7y)$ over $[-l, l] \times [-l, l]$ which is essentially the same as the solution obtained for $\mu = 25$ in 6.

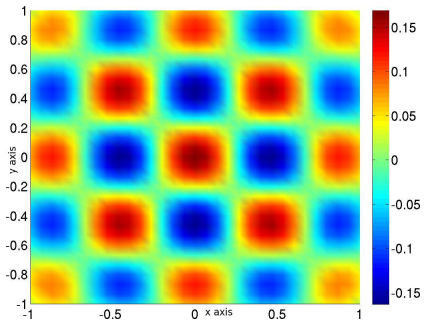

Figure 6: Plot of the solution of equation (2) at $T = 700$ for $n = 1$, $q = 2$, for the values $\xi_1 = 0.2$, $\xi_2 = 0.3$ and $A = 1$ in (11) with $\mu = 25$.

6 Conclusion

We have studied the existence, uniqueness, and asymptotic stability of a solution of nonlinear delay integro-differential equations that describe the spatio-temporal activity of sets of neural masses. We have also briefly presented an approximation and numerical scheme for one-dimensional models of two populations of neurons.

Using methods of functional analysis, we have found sufficient conditions for the existence and uniqueness of these solutions for general inputs. We have developed a Lyapunov functional which provides sufficient conditions for the solutions to be asymptotically stable. These conditions involve the connectivity functions and the slopes of the sigmoids as well as the time constant used to describe the time variation of the postsynaptic potentials.

We hope that our numerical schemes and experiments (see [5]) will lead to new and exciting investigations such as a thorough study of the bifurcations of the solutions of our equations with respect to such parameters as the slope of the sigmoid and the delays.

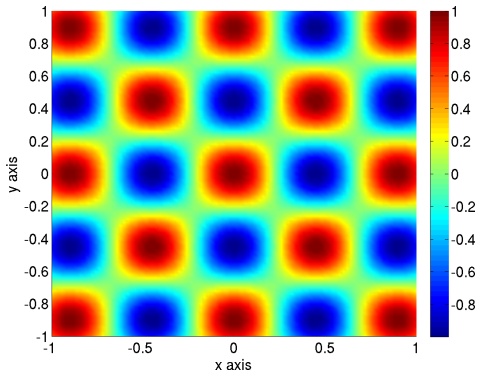

Figure 7: Plot of the function $(x, y) \mapsto \cos(7x)\cos(7y)$.

Acknowledgments
This work was partially funded by the ERC advanced grant NerVi number 227747.

References

[1] S.-I. Amari. Dynamics of pattern formation in lateral-inhibition type neural fields. *Biological Cybernetics*, 27(2):77–87, jun 1977.

[2] Fatihcan M. Atay and Axel Hutt. Stability and bifurcations in neural fields with finite propagation speed and general connectivity. *SIAM Journal on Applied Mathematics*, 65(2):644–666, 2005.

[3] S. Coombes and C. Laing. Delays in activity based neural networks. *Philosophical Transactions of the Royal Society A.*, 367:1117–1129, 2009.

[4] S. Coombes, N.A Venkov, L. Shiau, I. Bojak, D.T.J. Liley, and C.R. Laing. Modeling electrocortical activity through local approximations of integral neural field equations. *Physical Review E*, 76(5):51901, 2007.

[5] G. Faye and O. Faugeras. Some theoretical and numerical results for delayed neural field equations. *Physica D*, 2010. Special issue on Mathematical Neuroscience.

[6] J.K. Hale and S.M.V. Lunel. *Introduction to functional differential equations*. Springer Verlag, 1993.

[7] A. Hutt. Local excitation-lateral inhibition interaction yields oscillatory instabilities in nonlocally interacting systems involving finite propagation delays. *Physics Letters A*, 372:541–546, 2008.

[8] A. Roxin, N. Brunel, and D. Hansel. Role of Delays in Shaping Spatiotemporal Dynamics of Neuronal Activity in Large Networks. *Physical Review Letters*, 94(23):238103, 2005.

[9] N.A. Venkov, S. Coombes, and P.C. Matthews. Dynamic instabilities in scalar neural field equations with space-dependent delays. *Physica D: Nonlinear Phenomena*, 232:1–15, 2007.

[10] H.R. Wilson and J.D. Cowan. Excitatory and inhibitory interactions in localized populations of model neurons. *Biophys. J.*, 12:1–24, 1972.

[11] H.R. Wilson and J.D. Cowan. A mathematical theory of the functional dynamics of cortical and thalamic nervous tissue. *Biological Cybernetics*, 13(2):55–80, sep 1973.

[12] J. Wu. *Theory and applications of partial functional differential equations*. Springer, 1996.